Korean J. Chem. Eng., **22**(4), 591-598 (2005)

Characterization of Fractured Basement Reservoir Using Statistical and Fractal Methods

Jaehyeon Park, Sunil Kwon and Wonmo Sung†

Geoenvironmental System Engineering, Hanyang University, Seoul 133-791, Korea
(*Received 16 February 2005 • accepted 13 May 2005*)

Abstract−This study presents a characterization of fractured basement reservoir by using statistical and fractal methods with outcrop data, seismic data, as well as FMI log data. In the statistical method, fracture intensity and length have been calculated from various outcrop data. The optimum statistical distribution functions of fracture length for outcrops have been identified with the use of discriminant equation derived from Crofton's theory. The Fisher distribution constant, representing the fracture orientation, has been computed from FMI log data. With the statistical values and distribution functions, a 3D fracture network system has been generated. The result shows that there is no distinction in orientation of the fracture network system, and it excellently matches with the outcrop data. In the fractal method, fractal dimensions of fracture length and strike for the seismic fracture network in areal distribution were calculated; a greater value in fractal dimension means that the fracture network system has intensive fractal characteristics. Meanwhile, vertical distribution and dip angle of the fracture system have been evaluated from FMI log data. The resulting 3D fracture system presents that the overall strike and distribution of the fracture system are excellently matched with those of seismic data.

Key words: Fractured Basement Reservoir, Statistical Method, Fractal Method, FMI Log Data, Seismic Fracture Data

INTRODUCTION

A large proportion of the world's proven oil reserves have been found in the reservoir rock that is naturally fractured. In a recent book, Nelson [2001] gives a list of some 370 fields where natural fractures are important for production and a significant proportion are in basement rocks. The occurrence of naturally fractured basement reservoirs has been known within the hydrocarbon industry for many years, but because they have been generally regarded as non-productive, they have failed to draw the attention of exploration. Yet, they are commonly distributed in various petroliferous regions throughout the world. However commercial naturally fractured basement oil deposits have been found by accident, while looking for other types of reservoir; there are some suggestions that basement reservoir oil accumulations are not freaks to be found solely by chance but are normal concentrations of hydrocarbons obeying the rules of origin, migration and entrapment.

Most basement rocks are hard and brittle with very low matrix porosity and permeability; consequently, in this type of reservoir, fluid flow mainly depends on the secondary porosity. Secondary porosity may be divided into two kinds by origin: tectonic porosity (joints, faults, and fracture, etc.) and dissolution porosity (weathered zones, etc.). So, a greater understanding of the fracture distribution and connectivity within basement reservoir may prove to be the key tool for improved production management of this type of reservoir. To do this work, not only dynamic data analysis of well tests, being able to provide the information for large area, but also various kinds of static data analysis, which can characterize each fracture properties have been applied.

However, in some cases, where a large fracture system controls the fluid flow of a fractured reservoir, we cannot be solely dependent on average properties derived from dynamic data analysis. In this occasion, more reliable characterization can be possible with static analysis as well as well test analysis simultaneously [Sung et al., 2001; Kwon et al., 2001].

Static data include core analysis data acquired for drilling, data for location and direction of discontinuity, various log data, seismic data, and outcrop data found near the reservoir. Now then, one can evaluate fracture properties composed of fracture intensity, location, length, and orientation that can be expressed as dip and dip angle, by applying the static data either to the statistical method or fractal method.

Originally, the statistical method was suggested to simulate the behavior of discontinuous rock mass in an underground space, but it can also be applied to evaluate fracture networks in a reservoir. In order to express the fracture system by means of statistical functions and statistical values, several researches in this area have been examined as follows. The evaluating method for fracture intensity by surveying outcrop data with scan-line method or window sampling method has been investigated by a number of authors [Warburton, 1980; Phal, 1981; Priest, 1993; Mauldon, 1998; Zhang and Einstein, 1998]. Many distribution functions have been proven to be suitable for simulating the fracture orientation [Fisher, 1953], and also several studies in evaluating the fracture magnitude by defining suitable probability density function [Barton and Hsieh, 1989]. Now, if we can determine the suitable combination of statistical functions determined from fracture characteristics, then a 3D fracture network system can be generated in a reservoir, and recently only a few researches exist for full field study [Lapointe, 2002].

Fractal method has been applied for numerous areas in engineering and scientific phenomena after Mandelbrot discovered that the irregular-shaped seashore could be explained by fBm (fractional Brownian motion) [Mandelbrot, 1982]. In petroleum engineering,

†To whom correspondence should be addressed.
E-mail: wmsung@hanyang.ac.kr

Hewett applied a kind of fractal theory, so-called SRA (successive random addition) method to characterize heterogeneous reservoirs in 1986 [Hewett, 1986]. Recently, fractal theory has been employed to figure out the precise fractal dimensions of fracture properties [Babadagli, 2001], such as fracture length, orientation, and location, since many authors validated that the fracture network system shows fractal characteristics [Barton and Larsen, 1985; Lapointe, 1988].

This study reports two strategies, statistical and fractal methods, to quantify the characteristics of a fracture network system in an igneous fractured basement reservoir.

STATISTICAL METHOD

1. Statistical Analysis for Outcrop Data

Three different outcrop data found near the field and FMI (formation micro-imager) data acquired at wells were used as input data. Outcrop data were divided into Loc. 1, 2 and 3 and illustrated in Fig. 1. With these outcrop data, fracture intensity and statistical distribution function for fracture length were determined. The expression of fracture intensity is able to be classified into three kinds: linear, areal, and volumetric intensities. Generally, two types of surveying method have been used: scan-line sampling method, and window sampling method. In this study, we employed the window sampling method, and in this case fracture intensity can be written as [Mauldon, 1998],

$$\rho = \frac{N - N_T + N_C}{2WH} \quad (1)$$

where N_T is the number of transect fractures and N_C is the number of contained fractures. The categorizing method for the fracture system is also presented in Fig. 1. The surveying results for outcrop data are summarized in Table 1. The fracture intensities for each outcrop of Loc. 1, 2, and 3 are 2.43, 1.39, and 5.65 ea/m^2, respectively. By using the obtained fracture intensity, the total number of fractures in the objective area can be calculated.

Now, in order to determine the statistical distribution function of fracture length, it was assumed that the fracture length could be computed by some representative distribution functions which were already verified by several authors. Exponential, log-normal, and gamma distribution functions were proposed in this work. For three different distribution functions, the discriminant equation derived from Crofton's theory, is applied (D_D), and the discriminant equation is also calculated with outcrop data (D_R), then the difference of (D_R-D_D) is calculated. Finally, the minimum one is then selected as the most suitable distribution function of fracture length for the outcrop data. The calculated results are presented in Table 2, and the discrimination equations for the distribution functions are as follows [Villaescusa and Einstein, 1988; Zhang and Einstein, 2000].

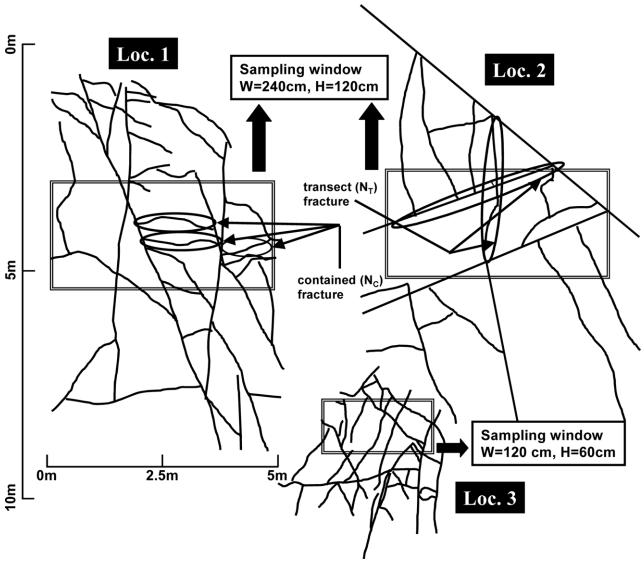

Fig. 1. Areal view of outcrop data, the setting of sampling windows, and two categories of fracture trace types.

Table 1. Summary of the analysis for fracture outcrop data

	Loc. 1	Loc. 2	Loc. 3
Total # of traces	32	24	60
Total length of all traces (m)	219.5	149.9	130.4
Mean trace length (m)	6.861	6.247	2.173
Standard deviation (σ, m)	5.089	5.504	1.412
Fracture intensity (ea/m^2)	2.43	1.39	5.56

Table 2. Determination of statistical distribution function for fracture length

Type	Distribution	Mean (m)	σ (m)	D_D (m)	D_R (m)	D_R-D_D (m)	Selection
Loc. 1	Actual trace	6.861	5.098	·	1,102.2	·	·
	Log-normal	2.873	3.506	788.6		313.5	selected
	Exponential	3.232	3.232	125.3		976.8	·
	Gamma	6.533	7.281	702.8		399.4	·
Loc. 2	Actual trace	6.247	5.504	·	251.7	·	·
	Log-normal	2.527	2.894	420.9		169.2	·
	Exponential	2.453	2.453	72.2		179.5	·
	Gamma	3.038	3.974	250.4		1.3	selected
Loc. 3	Actual trace	2.173	1.412	·	24.6	·	·
	Log-normal	1.371	1.095	22.1		2.5	selected
	Exponential	0.853	0.853	8.7		15.9	·
	Gamma	0.685	0.801	9.0		15.7	·

- Log-normal distribution function:

$$D_{log}=\frac{(\mu_D)^2+(\sigma_D)^{2^2}}{(\sigma_D)^8} \quad (2)$$

where,

$$\mu_D=\frac{2^7(\mu_l)^3}{3\mu^3(\mu_l)^2+(\sigma_l)^2}$$

$$\sigma_D=\frac{3\times 2^9\pi(\mu_D)^2+(\sigma_D)^2(\mu_D)^4-2^{14}(\mu_D)^6}{3^2\pi^6(\mu_D)^2+(\sigma_D)^{2^2}}$$

- Exponential distribution function:

$$D_{exp}=12(\mu_D)^2 \quad (3)$$

where,

$$\mu_D=\frac{2}{\pi}\mu_l$$

- Gamma distribution function

$$D_{gam}=\frac{(\mu_D)^2+2(\sigma_D)^2(\mu_D)^2+3(\sigma_D)^2}{(\mu_D)^2} \quad (4)$$

where,

$$\mu_D=\frac{2^6(\mu_l)^2-3\pi^2(\mu_D)^2+(\sigma_D)^2}{2^3\pi\mu_l}$$

$$\sigma_D=\frac{2^6(\mu_l)^2-3\pi^2(\mu_l)^2+(\sigma_l)^2}{2^6\pi^2(\mu_l)^2}\times\frac{3\pi^2(\mu_l)^2+(\sigma_l)^2-2^5(\mu_l)^2}{2^6\pi^2(\mu_l)^2}$$

FMI data, shown in Fig. 2, was used to evaluate fracture intensity. FMI can provide the information of fracture continuity and orientation along with the wellbore by using four image flaps. By analyzing FMI data on the basis of continuity of image flaps, we could verify five types of fractures, and among these, excluding discontinuous fractures, four types of fractures were chosen as effective fracture groups: continuous fracture, vuggy fracture, drilling-induced fracture, and healed fracture. After effective fractures were screened, the Fisher constant could be calculated by the information of dip and dip angle of the fractures which were obtained from FMI analysis. The Fisher constant represents the tendency of orientation of fracture groups, which can be described as follows: the greater the Fisher constant, the more identical the orientation of the fracture set. Although 463 fracture data were detected at the A-2X (ST) well, which was identified to have the largest number of effective fractures, 63 discontinuous fractures were discarded and only 394 effective fractures were used in this study. To calculate the Fisher constant, first, normal vectors and their resultant vectors were obtained and could be written as follows [Fisher, 1953],

$$\frac{e^x+e^{-x}}{e^x-e^{-x}}-\frac{1}{x}=\frac{|r|}{N} \quad (5)$$

where, x is Fisher constant.

The resulting Fisher constant of A-2X (ST) is 1.46, which indicates no distinctive directional trend of the fractures, and average dip and dip angle are 73.4, 176.3 degrees, respectively.

2. Construction of Fracture System Using Statistical Model

The target zone is Phase I area in field map shown in Fig. 3, and it has been identified to be 800 m thick and to be a fractured basement reservoir (Fig. 3). Phase I area was scheduled to be developed first in the field, and two production wells (A-1 and A-2X (ST)) have been drilled in this area. DST (drill stem test) data analysis indicates that fracture network system near the wellbore is considered to be the main fluid conduit in the reservoir.

A (4,500 m×2,500 m×800 m) size rectangular-shaped 3D space (Fig. 4) containing contain Phase I area was built. Total number of fractures from the fracture intensity were calculated in 3D space. That is, 1.407×10^7 ea/m^2 of fractures were generated. However, it is impossible to present the fractures in one chart because of nu-

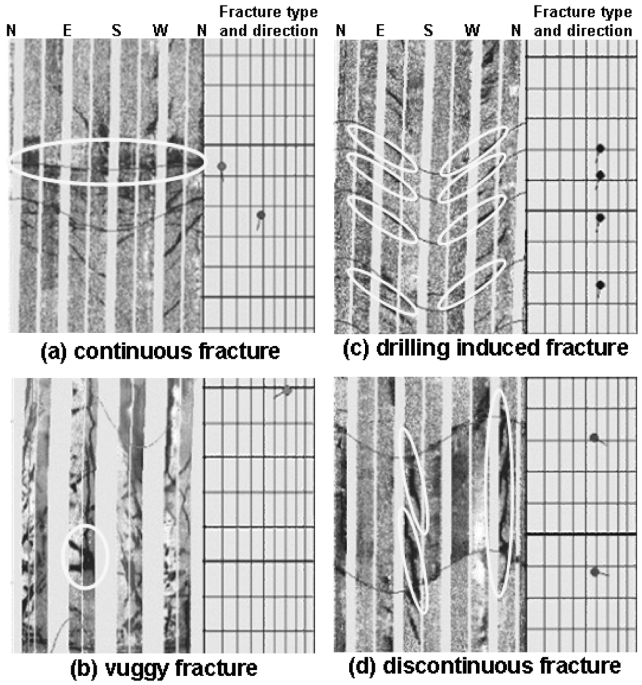

Fig. 2. Four types of fracture obtained by FMI data analysis.

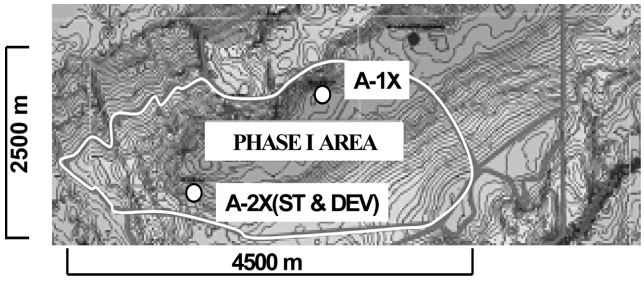

Fig. 3. Areal view of Phase I zone and well locations.

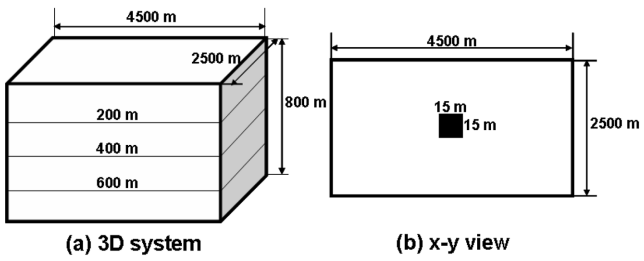

Fig. 4. 3D fracture generation system by statistical method.

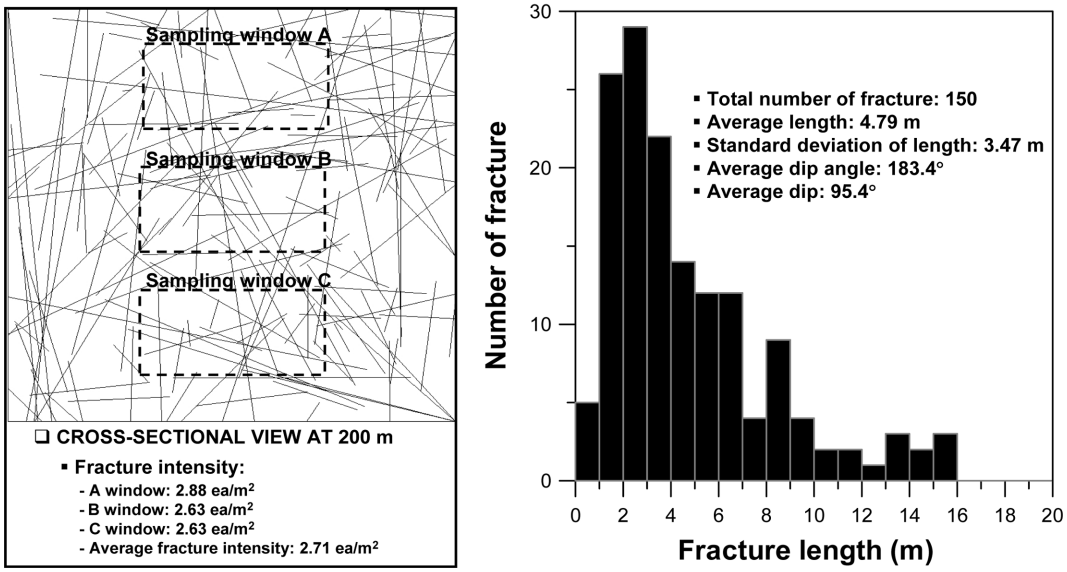

Fig. 5. Cross-sectional view at 200 m and statistical results.

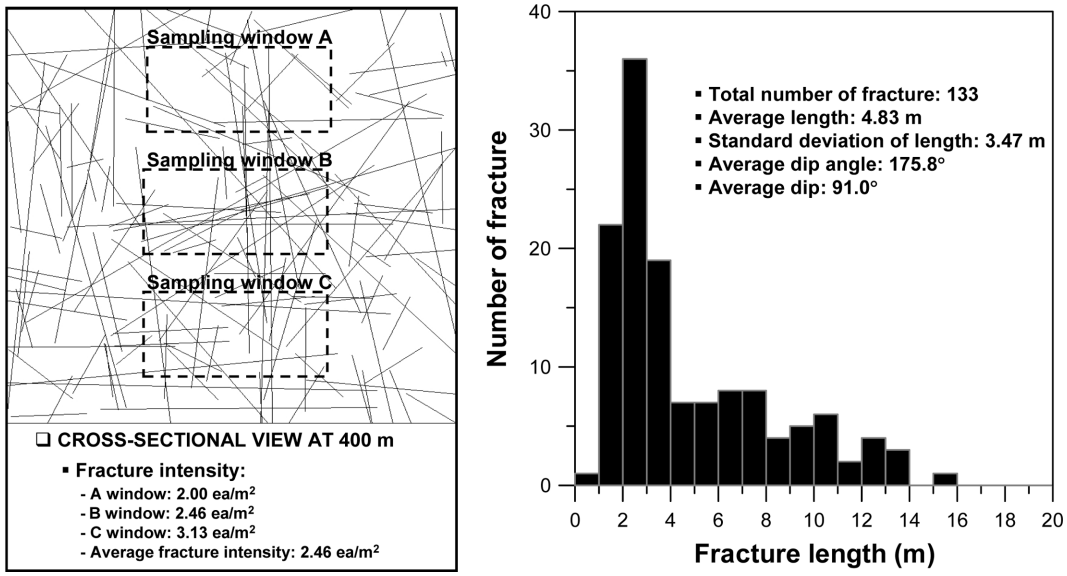

Fig. 6. Cross-sectional view at 400 m and statistical results.

merous numbers of fractures as well as short length of fracture compared to the size of the Phase I area. Thus, we selected a (15 m× 15 m) zone at the center, and the fracture profiles at the center zone of Phase I area were presented for the depths of 200 m, 400 m, and 600 m. As shown in Figs. 5 through 7, three sampling windows are set to evaluate the fracture intensity, and number of fractures, average fracture length, and fracture orientation information. As a result, the most fractures are 1 m to 4 m long, and there are only few fractures longer than 12 m. The result also shows that average fracture length at a depth of 600 m is 3.69 m, being the shortest, and 4.83 m, at 400 m, which is the longest. The resulting average dip angle varies from 175.8 to 183.4 degree, which matches well with the input data of 176.3 degree evaluated from FMI data. The dip was calculated in the range of 83.4 to 95.4 degrees, which is slightly greater than that of FMI data of 73.4 degree. The fracture intensity was calculated to be 2.46 through 3.04 ea/m^2, and it is coincident with the average intensity of outcrop data of 3.13 ea/m^2. At a depth of 200 m, fracture intensity does not vary much with the locations (2.63 through 2.88), while at depths of 400 m and 600 m, it was computed to be in a wider range with the locations (2.0 through 3.38 ea/m^2).

FRACTAL METHOD

1. 2D Fractal Formulation

Fractal sets can be characterized by using fractal dimension as

$$N = Cr^{-D} \tag{6}$$

where D is the fractal dimension.

While the dimension of Euclidean geometry is always expressed

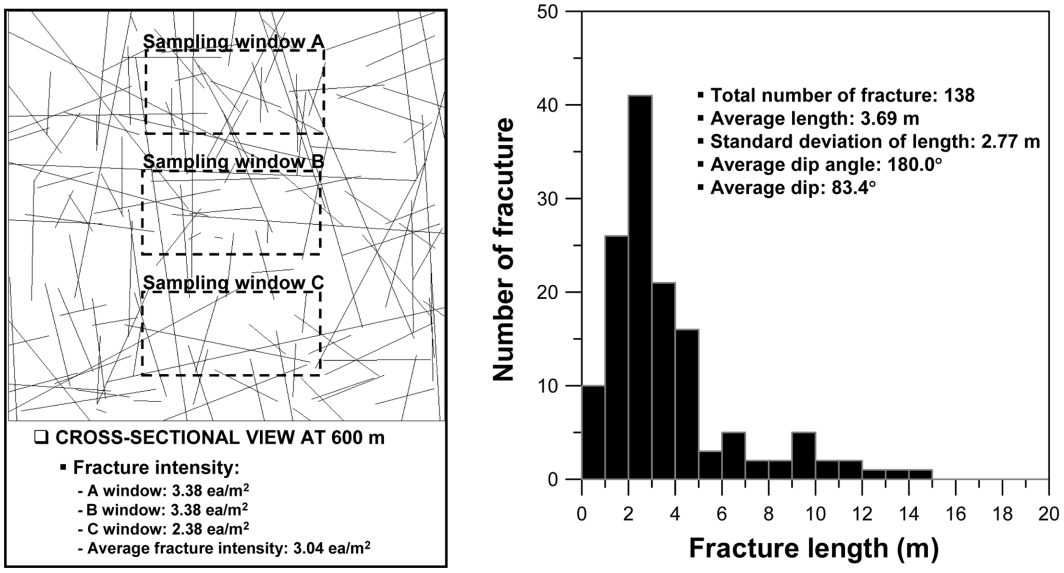

Fig. 7. Cross-sectional view at 600 m and statistical results.

as an integer, the fractal dimension could be a decimal fraction. Fractal dimensions were computed with the aid of a box-counting method [Kim et al., 2000; Chon and Choi, 2001] which can be inferred from Eq. (6). Once the fractal dimension is calculated, the properties of the fractal set can be created on the objective space by applying the transformation function which has been derived on the basis of typical fractal characteristics: self-affinity and self-similarity. The transformation function was developed on a simple basis of topology [Mathews et al., 1988]. Fig. 8 shows the procedure of transformation and compaction of original property. This procedure can be written as

$$w_i \begin{bmatrix} x \\ y \\ \phi \end{bmatrix}^{k+1} = \begin{bmatrix} a_i & b_i & c_i \\ d_i & h_i & k_i \\ l_i & m_i & j_i^* \end{bmatrix} \begin{bmatrix} x \\ y \\ \phi \end{bmatrix}^{k} + \begin{bmatrix} e_i \\ f_i \\ g_i \end{bmatrix} \tag{7}$$

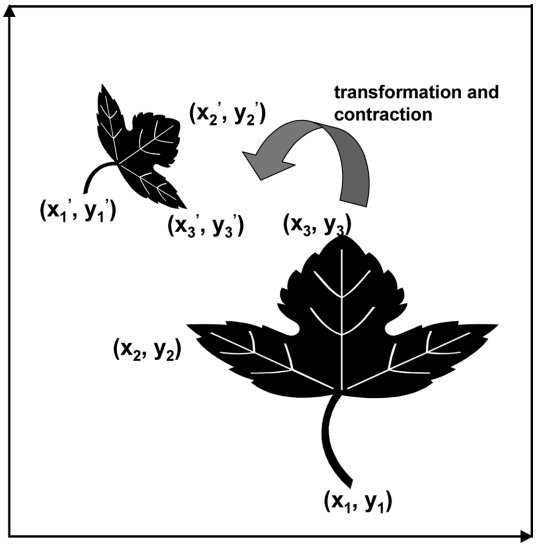

Fig. 8. Transformation and contraction between two leaves in an x-y space [Kim et al., 2000].

where i is the set of addresses of observation points, and coefficients ai through j_i^* can be determined by several constraint conditions and by the application of fractal dimensions [Barnsely, 1988]. The coefficients of a_i, b_i, d_i, and h_i compress areal space in the directions of x and y in accordance with the set of addresses of point i, and then e_i and f_i restrict the contracted points within the system to make it meaningful data. While c_i and k_i mean the effect of transformed fractal properties on the space, l_i and m_i evaluate the influence of space transformation over properties. In this study, c_i and k_i were assumed to be zero because these coefficients might be meaningless in reservoir conditions, and l_i and m_i were set to be equal in x-y direction. The coefficient g_i is also a constraint coefficient for fractal properties, and j_i^* is the property contraction factor to be evaluated by fractal dimension. The coefficient j_i^*, varying from zero to unity, will increase with greater fractal dimension and consequently the fractal properties can be transformed much more. The constraint conditions about each coefficient in Eq. (7) are summarized as follows:

$$\begin{bmatrix} c_i = k_i = 0 \\ a_i = h_i \\ l_i = m_i \\ b_i = -d_i \end{bmatrix} \tag{8}$$

Finally, an algorithm being able to generate fractal properties in reservoir, when Euclidean sets for addresses of observation points are selected, was suggested as follows:

$$\begin{bmatrix} x^{k+1} = a_i x^k + b_i y^k + e_i \\ y^{k+1} = -b_i x^k + a_i y^k + f_i \\ \phi^{k+1} = l_i x^k + l_i y^k + j_i^* \phi^k + q_i \end{bmatrix} \tag{9}$$

The subscript i in the above equation indicates the property relationship between the observation points. The set of addresses of observation points can be constituted to be irregularly as well as regularly as shown in Fig. 9. In this study, irregular type of set of

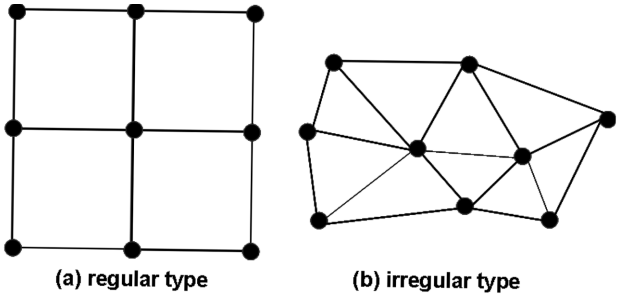

Fig. 9. General sets of addresses of points.

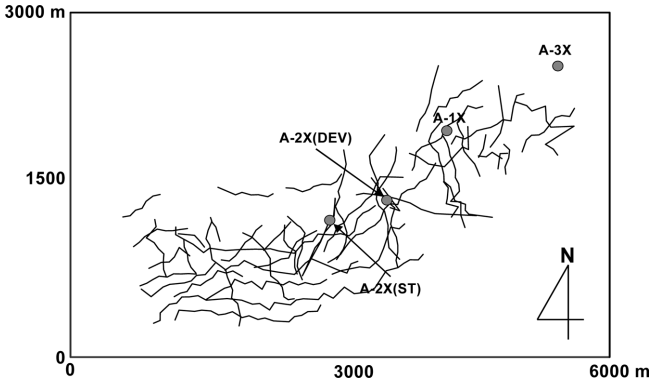

Fig. 10. Seismic data and well locations in Phase I area.

address points was utilized to increase the spatial relation among the fractal properties.

2. Construction of Fractal Fracture System Using Seismic Data

Unlike statistical analysis, seismic data (Fig. 10) was used as input data for the generation of a fracture system by using fractal method. From Fig. 10, the detected number of fractures was 171 within Phase I area. The x-y coordinates with length and strike of all fractures (171) were measured. Overall, the orientation of the fracture system is found to be NE-SW.

As a first step, fractal dimensions of fracture strike and length

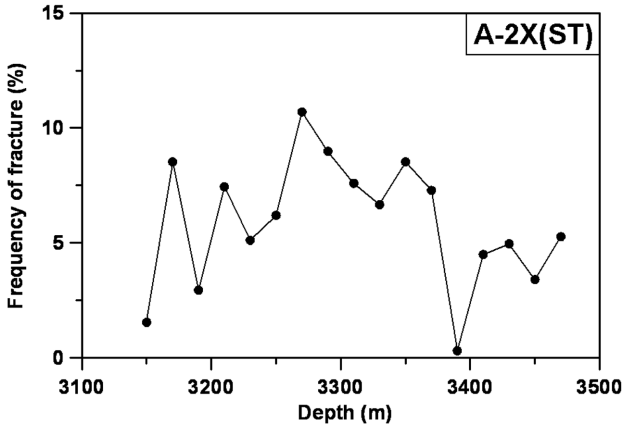

Fig. 12. The vertical distribution of fracture in A-2X (ST) well.

have been computed as 1.79 and 1.78, respectively, (Fig. 11). The calculated fractal dimensions are relatively closer to 2.0. Therefore, it can be concluded that the length and strike of the fractures have intensive fractal characteristics. By applying the fractal dimensions to Eq. (9), fracture strike and length were evaluated on 2D space with 464 irregular type set of addresses of points.

With the above areal information of the fracture system, vertical distribution of fractures was also applied by using FMI data. The vertical profile of fractures, including discontinuous type fractures in A-2X (ST), was analyzed and its results are presented in Fig. 12. Almost 80% of the fractures are distributed within 200 m thickness, from 3,200 m to 3,400 m, and as is the case for A-1X well and A-3X well nearby A-2X (ST). Hence, the fractures were generated more intensively in the interval of 3,200 m and 3,400 m. In fracture orientation, the dip can be easily computed, since the dip is perpendicular to the fracture strike which was already verified by fractal method. Meanwhile dip angle cannot be figured out by fractal method, and hence the Fisher constant and average dip angle were applied, which can be calculated by statistical methods. With the aid of 2D fractal results and the statistical values, fractures of 63550 were generated. As shown in Fig. 13, a fracture profile at a depth

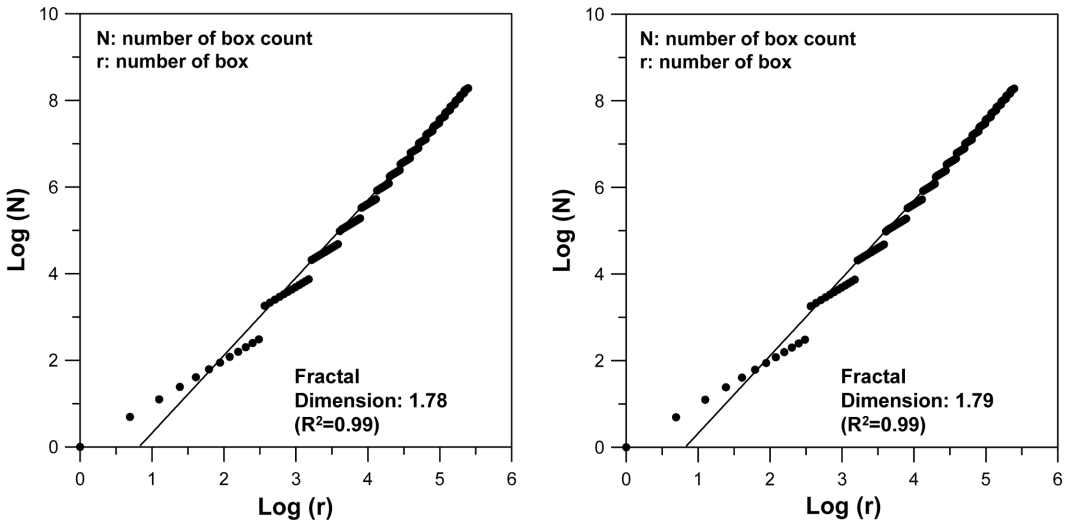

Fig. 11. Fractal dimensions of fracture length and fracture strike for seismic fracture data.

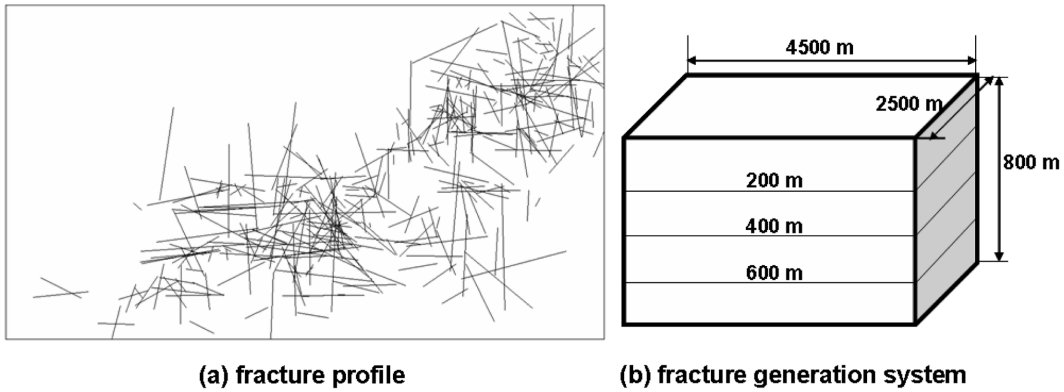

Fig. 13. Fracture profile in Phase I area at the depth of 400 m.

of 400 m was presented. From the result of Fig. 13, there are fractures of 1279, and these fractures were distributed along the NE-SW direction. This tendency of fracture orientation is well matched with that of input data. The result shows that the average fracture length is 271.5 m and it is much greater than that of the statistical method. In fracture orientation, average dip angle and dip are evaluated as 161.9 and 115.4 degrees, respectively. Also, the dip angle coincides with the average dip angle obtained by FMI data.

CONCLUSION

In the development of a fractured basement reservoir, it is essential to characterize the fracture network system in the reservoir intensively. In this study, two kinds of fracture evaluation method were presented by applying outcrop data, seismic fracture data and FMI data.

In the use of the statistical method for generating fracture network system, fracture intensity was calculated by window sampling method, and fracture orientation was evaluated from the Fisher constant. The fracture intensity was calculated as 2.46 to 3.04 ea/m^2 which is very comparable to average fracture intensity for outcrop data of 3.13 ea/m^2. The resulting average dip angles using the statistical method are in the range of 175.8 and 183.4 degrees, and it matches well with 173.6 degrees evaluated from FMI log analysis data.

This time, actual seismic fracture data was utilized for fractal analysis together with vertical distribution of fractures obtained by FMI log data. The results show that fractal dimensions for strike and length of fractures were estimated as 1.79 and 1.78, respectively, that is, those properties have intensive fractal characteristics. By using the fractal dimensions and FMI data, the fracture network system was generated in three dimensional space. The results present that the orientation of the fracture system appeared to be in the NE-SW direction, which is trend similar to seismic data. Also, one can note that the resulting dip angle coincides with that obtained by FMI data.

NOMENCLATURE

a, b, c, d, e, f, g, h, j, k, *l*, m : the coefficient of transformation function
D : discriminant equation
H : height of sampling window [m]
W : width of sampling window [m]
w : transformation function
γ : resultant vector
κ : Fisher constant
μ : average of fracture length
ρ : fracture intensity [ea/m^2]
σ : standard deviation of fracture length

Subscripts

C : contained fracture
D : distribution function
i : index of addresses points
T : transect fracture

REFERENCES

Babadagli, T., "Fractal Analysis of 2-D Fracture Networks of Geothermal Reservoir in South-Western Turkey," *Journal of Geothermal Research*, 112 (2001).

Barnsely, M. F., *Fractals Everywhere*, Academic Press, Newyork (1988).

Barton, C. C. and Hsieh, P. A., *Physical and Hydrologic-flow Properties of Fractures*, Field trip guide book T385, 28th Int. Geol. Cong., Washington DC (1989).

Barton, C. C. and Larsen, E., *Fractal Geometry of Two-Dimensional Fracture Networks at Yucca Mountain, South-Western Nevada*, Proceedings of International Symposium on Fundamentals of Rock Joints, Bjorkliden, Sweden (1985).

Chon, B. and Choi, Y., "Modeling of Three-Dimensional Groundwater Flow Using the Method to Calculate Fractal Dimension," *Korean J. Chem. Eng.*, **18**, 3 (2001).

Fisher, R. A., *Dispersion on Sphere*, Proc. of Royal Society London A217 (1953).

Hewett, T. A., *Fractal Distribution of Reservoir Heterogeneity and Their Influence on Fluid Transport*, paper SPE 15386 presented at the 61st Annual Technical Conference and Exhibition, New Orleans, LA (Oct. 1986).

Kim, I. K., Kang, J. S., Chang, S. W. and Choi, H. S., "Comparison of Regenerated Distribution Pattern of Deep-sea Bed Manganese Nodule Abundance Using Random Residual Addition and Fractal Geometry Transformation Procedure," *Korean Institute of Geology, Mining*

and Materials, **37**, 1 (2000).

Kwon, O. K., Ryou, S. S. and Sung, W. M., "Numerical Modeling Study for the Analysis of Transient Flow Characteristics of Gas, Oil, Water and Hydrate Flow through a Pipeline," *Korean J. Chem. Eng.*, **18**, 1 (2001).

Lapointe, P. R., "A Method to Characterize Fractal Density and Connectivity Through Fractal Geometry," *Int. J. Rock Mech. Min. Sci. Geomech. Abstr.*, 25 (1988).

Lapointe, P. R., *3D Reservoir and Stochastic Fracture Network Modeling for Enhanced Oil Recovery*, Circle Ridge Phosphoria/Tensleep Reservoir, Wind River Reservation, Arapaho and Shoshone Trives, Wyoming, Semi-Annual Report, U.S. DOE (2002).

Mandelbrot, B. B., *The Fractal Geometry of Nature*, W. H. Freeman and Co., Nework (1982).

Mathews, J. L., Emanuel, A. S and Edward, K. A., *A Modeling Study of the Mitsue Stage 1 Flood Using Fractal Geostatistics*, paper SPE 18327 presented at the 63rdAnnual Technical Conference and Exhibition, Houston, TX, (Oct., 1988).

Mauldon, M., "Estimating Mean Fracture Trace Length and Density from Observations in Convex Window," *Rock Mechanics and Rock Engineering*, **31**, 4 (1998).

Nelson, R. A., *Geologic Analysis of Naturally Fractured Reservoir*, Gulf Publishing Co. Book Division, 2nd Edition (2001).

Pahl, P. J., "Estimating the Mean Length of Discontinuity Traces," *Int. J. Rock Mech. Min. Sci. & Geomech, Abstr.*, **18** (1981).

Priest, S. D., *Discontinuous Analysis of Rock Engineering*, Chapman & Hall (1993).

Sung, W. M., Ryou, S. S., Ra, S. H. and Kwon, S. I., "The interpretation of DST data for Donghae-1 Gas Field, Block VI-1, Korea," *Korean J. Chem. Eng.*, **18**, 1 (2001).

Villaescusa, W. S. and Einstein, H. H., "Characterizing Rock Joint Geometry with Joint System Models," *Rock Mechanics and Rock Engineering*, **21** (1988).

Warburton, P. M., "A Stereogical Interpretation of Joint Trace Data," *Int. J. Rock Mech. Min. Sci. & Geomech, Abstr.*, **17**, (1980).

Zhang, L. and Einstein, H. H., "Estimating the Intensity of Rock Discontinuities," *Int. J. Rock Mech. Min. Sci.*, **37** (2000).

Zhang, L. and Einstein, H. H., "Estimating the Mean Trace Length of Rock Discontinuities," *Rock Mechanics and Rock Engineering*, **31**, 4 (1998).